

### 3. A new module to simulate surface crop residue decomposition: description and sensitivity analysis

Tommaso Tadiello<sup>a</sup>, Mara Gabrielli<sup>a\*</sup>, Marco Botta<sup>a</sup>, Marco Acutis<sup>a</sup>, Luca Bechini<sup>a</sup>, Giorgio Ragalini<sup>a</sup>, Andrea Fiorini<sup>b</sup>, Vincenzo Tabaglio<sup>b</sup>, Alessia Perego<sup>a</sup>

<sup>a</sup> Dipartimento di Scienze Agrarie e Ambientali Produzione, Territorio, Agroenergia, Università degli Studi di Milano, Milano, Italy

<sup>b</sup> Department of Sustainable Crop Production, Università Cattolica del Sacro Cuore, Via Emilia Parmense 84, 29122, Piacenza, Italy

\* Corresponding author, mara.gabrielli@unimi.it, tel. +39 02 5031 6612, via Celoria 2, 20133, Milano

#### Abstract

In the agroecosystem, the surface crop residues are widely recognized as affecting many processes such as soil water dynamics, crop growth, nitrogen and carbon cycling. For this reason, developing models that simulate the effect of the surface residues and their decomposition is crucial, especially while modelling conservation agriculture. To date, even though many cropping systems and C-oriented models differently simulate the evolution of the surface residue biomass, an integrated approach is still missing. In this study, we developed a new simulation module that explicitly simulates the decomposition of surface residues by including all variables and processes relevant to the agroecosystem's simulation. This module has been later integrated into the ARMOSA cropping system model. To quantify the contribution of each parameter to the simulated outputs (i.e., decomposed biomass), a sensitivity analysis (SA) was conducted, comparing the result with the APSIM model used as a benchmark. The SA was conducted on four different crop residues (maize, rye, soybean and wheat) over three different years. In addition, for each crop residue, the SA was performed for long and short simulation periods to verify whether parameters behaved differently according to the examined time period. The most critical parameters of the new module reflected the importance of the soil temperature, soil water content and residue biomass in the decomposition process. The potential decomposition rate had minor importance, highlighting that, when setting crop-specific values, other environment-related parameters are more relevant for the actual decomposition rate. In the case of APSIM model, the potential decomposition rate and the parameter related to soil temperature resulted in the first

two ranks. Finally, concordance coefficients were used to compare SA outputs: compared to APSIM, the new model showed higher concordance passing from one crop residue to another even when comparing the short and long simulation periods within the same crop. In summary, this work presented a novelty in the surface residue representation and provided a deep survey of the module behaviour and characteristics.

#### Keywords

Surface residues; crop residues; crop modeling; sensitivity analysis; conservation agriculture

#### Highlights

- A new simulation module has been developed to account surface residue decomposition;
- The new module has been later implemented into the ARMOSA model;
- A sensitivity analysis allowed to detect parameter/process importance;
- Soil temperature and water content, and residue mass mostly impact on decomposition;
- APSIM model has been used as a benchmark to test the new module.

### 3.1 Introduction

Surface crop residues represent a fraction of aboveground biomass lost by the crop through senescent organs or left on soil surface after harvest (for main crops) or termination (for cover crop). Permanent soil cover with surface crop residues is one of the main principles of conservation agriculture (FAO, 2016). Thus, leaving dead biomass on soil surface is considered as an important agronomic practice having a relevant impact on many processes such as soil water dynamics, soil erosion (Dietrich et al., 2019) and biodiversity, thus promoting crop growth and yield (Fiorini et al., 2020). Moreover, residue biomass retention and its subsequent decomposition has a significant effect on nitrogen and organic carbon dynamics (Chaves et al., 2021; Stella et al., 2019; Robertson et al., 2015; Iqbal et al., 2015; Coppens et al., 2007; Guérif et al., 2001). For these reasons, the development of models that estimate simultaneously the decomposition of surface crop residues and their consequent transformation into soil organic matter along with the water and crop dynamics is crucial for a proper assessment of matter and energy flows in agroecosystems (Moreno-Cornejo et al., 2014). Another reason to specifically simulate the surface residue degradation is the slower decomposition rate of this residue pool compared to the one incorporated into the soil (Douglas et al. 1980). To date, different cropping system models have been developed to simulate the decomposition of surface residues in response to pedoclimatic conditions and agronomic management. Besides the way they deal with the main environmental factors regulating the decomposition, each model differently focuses on specific

biochemical or physical characteristics of the process. For example, the EPIC model considers the residue biochemical structure (through the lignin content), splitting the residues into metabolic and structural compartments (Izaurre et al., 2006; Williams et al., 1984). The WEPP model carefully describes the effect of tillage operations on surface residues and considers standing and laying residues as two independent pools (Alberts et al., 1987). STICS is mainly based on nitrogen availability as regulating factor of residue decomposition rate (Justes et al., 2009; Brisson et al. 1998), while APSIM developed different approaches to model the slower decomposition of the upper part of the surface residue layer (Holzworth et al., 2014; Thorburn et al. 2001). All the models mentioned above also simulate several other processes that directly involve surface residues or are affected by their presence (among which the most relevant are residues' water retention and evaporation, C and N fluxes deriving from residue decomposition and soil covering effect).

On the other hand, a more detailed simulation of residue decomposition is carried out by many C-oriented models (Dietrich et al., 2017; Nendel et al., 2011; Bruun et al., 2006). Even though they can simulate the decomposition process in detail, the fact that they usually do not simulate crop growth, as well as the effect of management operations on soil physico-chemical properties, makes them less suitable for assessing the contribution of residues to agroecosystem functioning.

To date, despite the richness of processes and the diversity of algorithms employed by both cropping system and C-oriented models, an integrated approach for the simulation of surface residue decomposition is still missing. A more exhaustive simulation of decomposition can improve the outputs of cropping system models and allows to better evaluate how this process impacts on the whole agroecosystem. Thus, following an integrated approach, we developed a new simulation module that explicitly simulates the decomposition of surface residues by including all variables and processes that are relevant for agroecosystems simulation and that can be resumed as: (i) main crop residues decomposition after harvest, (ii) cover crop residues decomposition after mechanical termination, (iii) senescent leaves accumulation/decomposition during crop growth. This last process is essential since senescent leaves represent a possible source of soil C (Rumpel,

2011) and N that persists on the soil for a significant time. This module has been integrated and tested within the ARMOSA cropping system model (Valkama et al. 2020; Perego et al., 2013).

An assessment of models based on sensitivity analysis (SA) is needed to quantify the contribution of each parameter to the simulated outputs (Richter et al., 2010); for this reason, SA is an essential step before model calibration. Furthermore, SA is helpful to understand the behavior of the models itself (Confalonieri et al., 2012) by identifying where (i.e., for which parameters) a reduction of uncertainty leads to the biggest reduction of the respective output uncertainty (Diel and Franko, 2020). This indicates where further efforts for data quality shall be put to best use (Saltelli et al., 2007). In addition, to our knowledge, there is a lack of comparison studies among cropping system models that use different approaches to simulate surface residue decomposition. Comparing the results of SA of different models is a common way to highlight models' agreements and dissimilarities for a deeper analysis of the process under evaluation.

Therefore, the objectives of this work were: (i) to develop an integrated new module and assess it within the ARMOSA model to simulate surface residue decomposition and the processes influenced by the residue presence; (ii) to assess the new module by analyzing its sensitivity to key parameters, in a case study with different crop residues and seasons; (iii) to compare the sensitivity analysis of the new module with that of the APSIM model, based on the same case study.

## 3.2 Materials and Methods

### 3.2.1 The APSIM approach

APSIM was developed to simulate biophysical processes in agricultural systems (Holzworth et al., 2014).

Decomposition of surface residues in APSIM is implemented through the so-called SurfaceOM module. It models the kinetics of decomposition of organic materials left on soil surface until they are incorporated with tillage. The module simulates the flow of C to soil pools following the decomposition of dead aboveground biomass (Meier and Thorburn, 2016; Thorburn et al. 2001) using first-order kinetics. The actual decomposition rate of the flat mass per unit area is obtained decreasing the potential decomposition rate (unique for the whole mass) through multiplicative factors (0-1) accounting for the limitations imposed by residue moisture, temperature, residue C:N ratio and residue-soil contact. The moisture factor is estimated

from the potential soil evaporation cumulated along the decomposition period. The effect of temperature on residue decomposition is described based on the average air temperature. The limiting C:N ratio is calculated using the C:N ratio of each individual residue type, even in case of different residues mixture. Lastly the residue-soil contact factor is applied where large amounts of surface residues are present, reducing the overall rates of decomposition.

### 3.2.2 The new surface residue decomposition module

The new surface residue decomposition module implemented in ARMOSA represents the most important processes regarding the dynamics of surface residue decomposition (biomass partitioning between standing and laying residues, decomposition rate and residue soil covering), and their influence on surface water balance (residue water retention and residue influence on soil evaporation) and soil properties (e.g., carbon and nitrogen balance). All the equations of the module are reported in Appendix A. After crop harvest or cover crop termination, the module simulates the actual decomposition rate of standing and flat residues separately. The decomposition process is based on different species-specific potential decomposition rates ( $PDR_s$  for standing residue biomass,  $PDR_f$  for flat residue biomass and  $PDR_f(\text{leaves})$  specifically for leaves belonging to the flat biomass) and is affected by environmental and management conditions.

We adopted some key processes from the WEPP model for the simulation of: 1) the partitioning of crop residues at harvest in standing and flat components, based on crop and cutting height; 2) the decomposition of the standing biomass (as a function of rain and temperature) and its conversion to the flat biomass (due to the action of wind and snow); 3) the soil covering level provided by standing and flat residues, possibly affected by soil tillage operations.

The decomposition of the flat component of surface biomass employs APSIM algorithms: the potential decomposition rate of surface residues is limited by temperature, C:N ratio of the residues, soil-residues contact degree, and soil moisture. These regulating factors act separately on the actual decomposition rate of the three (stand, flat and leaves) pools. Unlike APSIM, however, the new module discriminates between leaf and stem biomass to account for their different susceptibility to decomposition. The effect of soil moisture was modelled based on the ARMOSA soil moisture simulation to be consistent with the algorithm

already implemented for the residues incorporated into the soil. Carbon and nitrogen fluxes from surface residues decomposition are allocated into stable soil carbon and mineral soil nitrogen. Lastly, the STICS approach was adopted for estimating residue water retention (limited by incident rainfall and influenced by residue wettability), assessing residue evaporation demand (based on the flat residue soil cover) and subsequently adjusting soil evaporation to fulfil the unsatisfied evaporation request.

### 3.2.3 Case study for sensitivity analysis

The scenario used for sensitivity analysis spans between 2013 and 2017 and is based on a long-term field experiment (started in 2011) at the CERZOO research station, in Piacenza (45°00'18.0" N, 9°42'12.7" E; 68m above sea level), Po Valley, Northern Italy. The soil at the field site is a fine, mixed, mesic Udertic Haplustalfs (Soil Survey Staff, 2014). Main soil (0-30 cm) properties before the beginning of the experiment were: organic matter content 21 g kg<sup>-1</sup>; pH (H<sub>2</sub>O) 6.8; bulk density 1.36 g cm<sup>-3</sup>; sand 122 g kg<sup>-1</sup>; silt 462 g kg<sup>-1</sup>; clay 416 g kg<sup>-1</sup>; soil total N 1.2 g kg<sup>-1</sup>; available P (Olsen) 32 mg kg<sup>-1</sup>; exchangeable K (NH<sub>4</sub><sup>+</sup> Ac) 294 mg kg<sup>-1</sup>, and cation exchange capacity 30 cmol<sup>+</sup> kg<sup>-1</sup>. The climate is temperate (Cfa Köppen classification), with an average annual temperature of 14.2 °C and annual rainfall of 778 mm (last 20-years average). Daily weather inputs required by the models were obtained by the Agri4Cast Resources Portal (Biavetti et al., 2014).

Briefly, the crop sequence was a three-year crop rotation: maize (*Zea mays* L.), soybean (*Glycine max* (L.) Merr.) and winter wheat (*Triticum aestivum subsp. aestivum* L.). Rye (*Secale cereale* L.) was utilized as a cover crop after maize and winter wheat, in a no-tillage regime. The experimental design was a randomized block with 4 replicates. Approximately two weeks before sowing the cash crop, cover crops were terminated by spraying Glyphosate [N-(phosphonomethyl) glycine] at the rate of 3 L ha<sup>-1</sup>. Cash crop and cover crop residues, after harvesting and termination respectively, were left onto the soil surface without chopping.

In this experiment, a residue biomass decomposition assessment was conducted on surface residue biomass of the cash crop and on the whole surface cover crop biomass. The different residues biomasses were used to initialize the models under the present study. Thus, the residue biomass from the harvest of the cash crop and from the termination of the cover crop represent the dependent variable on which the present study is based. We will use the term "surface residue biomass" for the biomass laying on the soil surface regardless of its source (i.e. harvest or termination). Once a cash or cover crop was harvested or terminated, the

residues of the previous crop (if still present on the surface) were removed from the soil, and the new residues were put on the soil surface. The removal of the previous residues from the soil (belonging to the previous cash crop at cover crop termination or belonging to cover crop at cash crop harvest) allowed to study the decomposition of one type of residue alone (cover or cash crop residues) instead of the decomposition of a residue mixture. More details about the whole experiment are available in Boselli et al. (2020).

#### 3.2.4 Sensitivity analysis

Sensitivity analysis (SA) was carried out on the amount of decomposed residue biomass, which is the dependent variable that is affected by all processes included in the new module. Therefore, all the parameters involved in biomass decomposition were considered in the sensitivity analysis. A complete parameters list is reported in Table 1.

To better assess the role of the parameters on the decomposition dynamics under different pedo-climatic conditions, several SAs were conducted on residues of all crops in the rotation, in the periods of the year when they are on the soil surface. In addition, for each tested crop, two timespans of decomposition, hereafter reported as "simulation periods", were considered: (1) the "Long Simulation Period" (LSP), from crop harvest/termination to the following crop harvest/termination, and (2) the "Short Simulation Period" (SSP), that is half of the long simulation period and starts from the same crop harvest/termination date (as reported in Figure 1). The introduction of the LSP and SSP periods allowed us to detect possible patterns of parameter sensitivity in different stages of residue decomposition. In fact, the analysis of SSP and LSP can distinguish the parameters that are important only at the beginning of the decomposition process (when the environmental conditions might be different compared to the end of LSP), from the parameters that maintain their importance along the whole decomposition period.

For both the new module and APSIM, the total number of SAs (10) was equal to the combination of the number of crops in the rotation (i.e., maize, rye, soybean, wheat, and rye) multiplied by the number of simulation periods (LSP and SSP). For each SA, Table 2 shows the specific crop residues under decomposition and the period of the year involved. Table 2 also shows the initial residue biomass at the beginning of each SA, that was derived from Boselli et al. (2020).

Table 1. Crop parameters selected for the sensitivity analysis. Equations related to the new module implementation are reported in appendix A.

Model	Name	Unit	Mean (SD)				Definition	Source
			Maize	Wheat	Rye	Soybean		
New module implemented in ARMOSA	PDR <sub>f</sub>	kg m <sup>-2</sup> d <sup>-1</sup>	0.0065 (0.00195)	0.0085 (0.00255)	0.0085 (0.00255)	0.0038 (0.0039)	Decomposition rate of the flat residue biomass	Calibrated starting from Stott et al., 1990 and Probert et al., 1998
	PDR <sub>f</sub> (leaves)	kg m <sup>-2</sup> d <sup>-1</sup>	0.015 (0.0045)	0.015 (0.0045)	0.015 (0.0045)	0.013 (0.0045)	Decomposition rate of the flat residue biomass (leaves)	Calibrated starting from Stott et al., 1990
	CN <sub>opt</sub>	-	25 (7.5)	25 (7.5)	25 (7.5)	25 (7.5)	Optimum C/N ratio of flat biomass for decomposition	Thorburn et al., 2001
	CN <sub>slope</sub>	-	0.277 (0.0831)	0.277 (0.0831)	0.277 (0.0831)	0.277 (0.0831)	Slope of C/N ratio function curve	Thorburn et al., 2001
	T <sub>opt</sub>	°C	20 (6)	20 (6)	20 (6)	20 (6)	Optimum temperature for decomposition	APSIM default values
	C <sub>ft</sub>	m <sup>2</sup> kg <sup>-1</sup>	2.1 (0.63)	6.4 (1.92)	6.4 (1.92)	5.2 (1.56)	Area to mass ratio of residue biomass	Stott et al, 1990
	B <sub>f_crit</sub>	kg m <sup>-2</sup>	0.2 (0.06)	0.2 (0.06)	0.2 (0.06)	0.2 (0.06)	Critical flat residue biomass above which the decomposition is slower	APSIM default values
	Wett <sub>mulch</sub>	mm Mg <sup>-1</sup> ha	2.6 (0.78)	2.6 (0.78)	2.6 (0.78)	2.6 (0.78)	Residue biomass water retention	Scopel et al., 1998
	SWC <sub>min</sub>	-	0.2 (0.06)	0.2 (0.06)	0.2 (0.06)	0.2 (0.06)	Minimum residue water content for decomposition	Calibrated
	SWC <sub>optmin</sub>	-	0.6 (0.18)	0.6 (0.18)	0.6 (0.18)	0.6 (0.18)	Minimum optimum residue water content for decomposition, expressed as a proportion of field capacity	Calibrated
	SWC <sub>optmax</sub>	-	1.1 (0.33)	1.1 (0.33)	1.1 (0.33)	1.1 (0.33)	Maximum optimum residue water content for decomposition expressed as a proportion of field capacity	Calibrated
	MA <sub>optb</sub>	-	1.5 (0.45)	1.5 (0.45)	1.5 (0.45)	1.5 (0.45)	First slope of the water limitation function	Calibrated
	MA <sub>opta</sub>	-	1 (0.3)	1 (0.3)	1 (0.3)	1 (0.3)	Second slope of the water limitation function	Calibrated
Conv <sub>ft</sub>	-	0.99 (0.297)	0.99 (0.297)	0.99 (0.297)	0.99 (0.297)	Adjustment factor to account for the effect of wind and snow on the standing residue biomass	Stott et al., 1990	
APSIM	B <sub>f_degr</sub>	kg m <sup>-2</sup> d <sup>-1</sup>	0.1 (0.03)				Potential decomposition rate (for all biomass)	APSIM default values
	CN <sub>opt</sub>	-	25 (7.5)				Optimum C/N ratio of residue biomass for decomposition	APSIM default values
	CN <sub>slope</sub>	-	0.277 (0.0831)				Slope of C/N ratio function curve	APSIM default values
	T <sub>opt</sub>	°C	20 (6)				Optimum temperature for decomposition	APSIM default values
	C <sub>ft</sub>	ha kg <sup>-1</sup>	0.0005 (0.00015)				Area to mass ratio of residue biomass	APSIM default values
	B <sub>f_crit</sub>	kg ha <sup>-1</sup>	2000 (600)				Critical mass of residue biomass above which the decomposition is slower	APSIM default values
	cum_eos_max	mm	20 (6)				Cumulative potential soil evaporation at which decomposition rate becomes zero	APSIM default values



Table 2. Simulation starting and ending dates for each crop residue in the rotation. The ending dates are divided between short (SSP) and long (LSP) simulation period. For each crop the initial total residues biomass is reported.

Crop residues	Simulation starting date (harvest or termination date)	Simulation ending date		Initial residue biomass (kg DM ha <sup>-1</sup> )
		SSP	LSP	
Maize	17/09/2014	07/01/2015	28/04/2015	11707
Rye (1)	21/04/2015	25/06/2015	28/08/2015	2850
Soybean	01/10/2015	29/01/2016	28/05/2016	3280
Wheat	08/07/2016	16/11/2016	27/03/2017	7577
Rye (2)	07/04/2017	13/06/2017	19/08/2017	2230

In addition, a comparison among crop residues decomposing in a similar period of the year was done to better evaluate the role of environmental conditions on decomposition: we have distinguished crop residues that decompose during the colder season (winter or fall) and residues that decompose during the warm season (spring or summer).

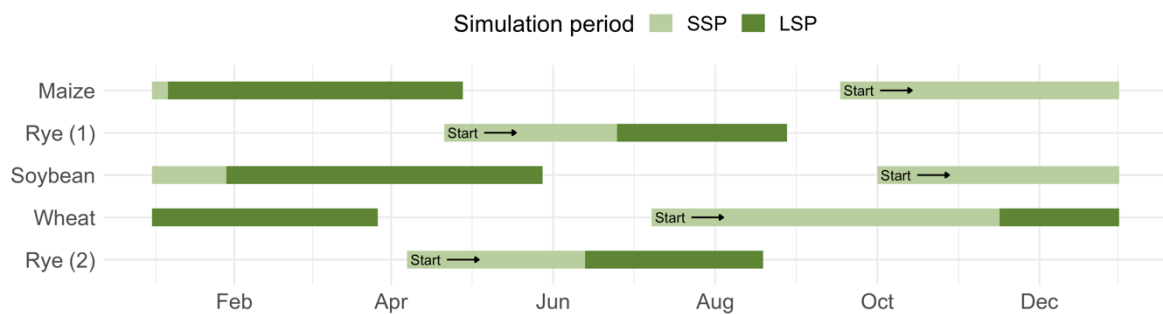


Figure 1. Simulation periods, Short Simulation Period (SSP) and Long Simulation Period (LSP), used for sensitivity analysis for each crop in the rotation.

Sensitivity analysis requires setting the average and standard deviation of the parameters. Parameters values were derived from the literature (Table 1). When no data were available, default or calibrated values were adopted. Standard deviation was set to 30% of the average for all parameters to prevent unrealistic values. All parameter distributions were assumed to be normal (Confalonieri et al., 2006).

Random variates of the same parameters were generated using the sampling technique for sensitivity analysis known as the Morris method (Morris, 1991) and further improved by Campolongo et al. (2004). This technique deals efficiently with models containing a large number of input parameters without relying upon strict assumptions about the model such as additivity or monotonicity of the input-output relationship (Confalonieri, 2006). The study of Paleari et al. (2021) highlighted that the Morris method is a suitable

alternative to more demanding SA methods (e.g., Sobol method) when ranking parameters or discriminating between influential and non-influential parameters.

The Morris method is based on a systematic sampling of the multidimensional space defined by the possible values of the parameters to generate a random set of OAT (i.e., once at time) experiments (Pianosi et al., 2016) and identifying the few crucial parameters based on the distribution ( $F_i$ ) of the elementary effect associated with the  $i^{\text{th}}$  input factor. To estimate these quantities, Morris suggests sampling  $r$  elementary effects from each  $F_i$  via an efficient design that constructs  $r$  trajectories of  $(k + 1)$  points in the input space, each providing  $k$  elementary effects, one per input factor.

For each model input ( $X$ ), the elementary effect is defined as:

$$d_i(X) = \left( \frac{y(X_i, \dots, X_{i-1}, X_i + \Delta, X_{i+1}, \dots, X_k) - y(X)}{\Delta} \right) \quad [1]$$

where (i)  $X = (x_1, \dots, x_k)$  as the  $k$ -dimensional vector of model studied parameters  $x_i$ ; (ii) all variables are rescaled in the 0–1 range; (iii)  $x_i$  can take only  $P$  (the number of levels, using the Morris terminology) discrete values in the set  $\{0, 1/(P - 1), 2/(P - 1), \dots, 1\}$  and (iv)  $\Delta$  is a multiple of  $1/(P - 1)$ .

The total cost of the experiment is thus  $r(k + 1)$  (Campolongo et al 2007). The Morris method requires the choice of the number of trajectories (sequences of points starting from a random base vector in which two consecutive elements differ only for one component) and levels. For both models, the sensitivity analysis was run using 10 trajectories and 4 levels.

The method samples values of  $X$  from the hyperspace  $\Omega$  (identified by an  $k$ -dimensional  $P$ -level grid) and finally calculates the mean ( $\mu$ , strength) assessing the overall influence of the parameter on  $y(X)$  and its standard deviation ( $\sigma$ , spread) estimating the totality of the higher order effects (Richter et al., 2010). In this work,  $\mu$  is considered as absolute value ( $\mu^*$ ) as proposed by Campolongo et al. (2004). The  $\mu^*$  value is successful in ranking parameters in order of importance and performs well when the goal is identifying non-influential parameters (Confalonieri et al., 2006). The second measure ( $\sigma$ ) is useful to detect parameters involved in interaction with other parameters, or whose effect is non-linear (Saltelli et al., 2004). With this

convention the more “dangerous” (i.e., sensitive) parameters are in the top right quadrant of the  $\sigma$  versus  $\mu^*$  plot (“danger zone”), where both sensitivity and strength are high (Confalonieri et al., 2006).

For the new module, the SA was conducted using the ARMOSA integrated feature that allows the model to easily interact with the Salib external library (Herman and Usher, 2017). This library implements many sensitivity analysis methods, including Morris. In the case of APSIM, the "sensitivity" package (Iooss et al., 2021) was used to setting the grid for the SA (i.e., a data frame with the combinations of parameters to be evaluated). To use this package the complementary "apsimx" package (Miguez, 2022) interface was utilized to set and run the SA. The functions belonging to the "apsimx" package also allow the user to open, inspect, read and edit the simulation file (.apsim). In addition, this package allows editing the configuration files (.xml), where the default setting of the parameters is stored. The code used to set the SA is available as supplemental material (Supplemental material 1).

### 3.2.5 Statistical analysis

To evaluate the agreement between the different sensitivity rankings within each model, the top-down concordance coefficient was applied, which allows to emphasize the agreement among rankings assigned to important parameters through the transformation of original data into Savage-scores (Savage, 1954). Savage-scores are calculated as follows:

$$S_i = \sum_{j=1}^n \frac{1}{j} \quad [2]$$

where  $i$  is the rank assigned to the rank  $i^{\text{th}}$  order statistic in a sample of size  $n$ . The  $i^{\text{th}}$  rank has been assigned to the different  $\mu^*$  for each parameter in a single SA.

After the conversion into Savage-scores, the Kendall's coefficient of concordance was applied. This coefficient of concordance can be used to measure the agreement among  $b$  sets of rankings when  $b > 2$  (Iman and Conover, 1987). It is also known as the top-down correlation coefficient because of its sensitivity to agreement among the top ranks. It can be computed as:

$$C_T = \frac{1}{b^2(n-S_1)} \sum_{i=1}^n S_i^2 - b^2n \quad [3]$$

where  $S_i$  is the sum of the Savage-scores assigned to the  $i^{\text{th}}$  object taken over all  $b$  sets of rankings. The coefficient of concordance is associated with a  $p$ -value under the Kendall null hypothesis that the  $p$  judges or

raters (i.e., set of SAs) produce independent rankings of the objects or subjects (i.e., parameters). To preserve the correct Type I error, Siegel and Castellan (1988) recommended the use of a permutation-based table of critical values for  $C_T$  only when the number of parameters is  $\leq 7$ . When the number of parameters exceeds seven, they recommended using the  $\chi^2$  distribution approximation. Thus, according to the parameters number, the *p-value* of each coefficient of concordance was obtained with the  $\chi^2$  distribution for the new module (14 parameters evaluated) and with the permutation-based method for APSIM (7 parameters evaluated) (Legendre et al., 2005). Both the  $C_T$  and the *p-values* coefficients were automatically retrieved from all sets of ranks using the R package "synchrony" (Tarik, 2019) using the ranking ties correction when necessary.

### 3.3 Results

#### 3.3.1 Models' parameters: similarities and differences between the new module and APSIM

The two modelling approaches (i.e., the new module and APSIM) utilized different parameters to simulate surface residue biomass decomposition (Table 1; Appendix A). Only five of them,  $CN_{opt}$  and  $CN_{slope}$  (accounting for the CN ratio of the residue biomass),  $T_{opt}$  (accounting for the optimal temperature for decomposition),  $Cf_{rt}$  (accounting for the area to mass ratio of residue biomass) and  $B_{f\_crit}$  (accounting for the critical flat residue biomass above which the decomposition is slower) are in common since they have the same biological meaning and role within the simulated process.

Other parameters reflect the different approaches adopted. Starting from the potential decomposition rates, the new module uses two different parameters, one for leaves ( $PDR_f(\text{leaves})$ ) and one for the rest of flat biomass ( $PDR_f$ ). These potential decomposition rates are further defined specifically for each crop. The third potential decomposition rate ( $PDR_s$ ) was not used in this study because of the lack of standing residue. APSIM instead uses a single potential decomposition rate ( $B_{f\_degr}$ ) regardless the residue biomass component. The limitation of biomass decomposition due to soil water is represented by four parameters in the new module ( $SWC_{min}$ ,  $SWC_{optmin}$ ,  $SWC_{optmax}$ ,  $MA_{optb}$  and  $MA_{opta}$ , Eq. 10, Appendix A, Table 1), whereas only by one parameter ( $cum\_eos\_max$ ) in APSIM. Furthermore, the new module uses the  $Wett_{mulch}$  and the  $Conv_{fct}$  parameters to

define the residue biomass water retention and to account for the effect of wind and snow on the standing residue biomass, respectively.

Other model parameters belonging to ARMOSA are not included in this analysis because they are not directly related to decomposition and were left at their default value.

### 3.3.2 Sensitivity analysis

Sensitivity analysis results are described separately for the new module and for APSIM. Within each of these approaches, SA results are presented for each crop in the rotation.

#### *New decomposition module implemented in ARMOSA*

The results differed based on the crop and the period of the year in which residues decompose. In the case of maize,  $T_{opt}$ ,  $B_{f\_crit}$  and  $SWC_{min}$  had the highest effect on decomposition, with no differences between SSP and LSP (top right quadrant in Figure 2A/2B). Another important parameter involved in the process was  $CN_{opt}$ , while all the other parameters had  $\mu^*$  equal or close to zero (Fig. 2A/2B).

For rye, a clear pattern was visible only in 2017 ("Rye (2)", Fig. 2I/2L) when the  $SWC_{min}$  (i.e., minimum residue water content for decomposition process expressed as a proportion of field water capacity) showed constantly a more relevant effect than all the other parameters. In 2015 (i.e., "Rye (1)"), the same pattern appeared only in LSP (Fig. 2D). In SSP (Fig. 2C) instead,  $B_{f\_crit}$  and  $T_{opt}$  appeared in the top right quadrant together with  $SWC_{min}$ . The impact of these three parameters could be discriminated by ranking on the basis of  $\sigma$ :  $T_{opt}$  maintained an essential role but its interactions with other parameters were low.

In the case of soybean,  $T_{opt}$  still had the same importance as found in maize. No other parameters had a significant influence on model outputs as indicated by low  $\mu^*$  (Fig. 2E/2F). For wheat, SA showed a clear pattern in SSP, with  $SWC_{min}$  covering the largest  $\mu^*$  percentage compared to all the other parameters (Fig. 2G). Values of  $\mu^*$  decreased smoothly in LSP from right to left but with discontinuities, allowing to distinguish the most influential parameters.  $SWC_{min}$  ranked first, followed by  $B_{f\_crit}$ ,  $T_{opt}$ ,  $SWC_{optmin}$  and  $PDR_f$  (Fig. 2H).

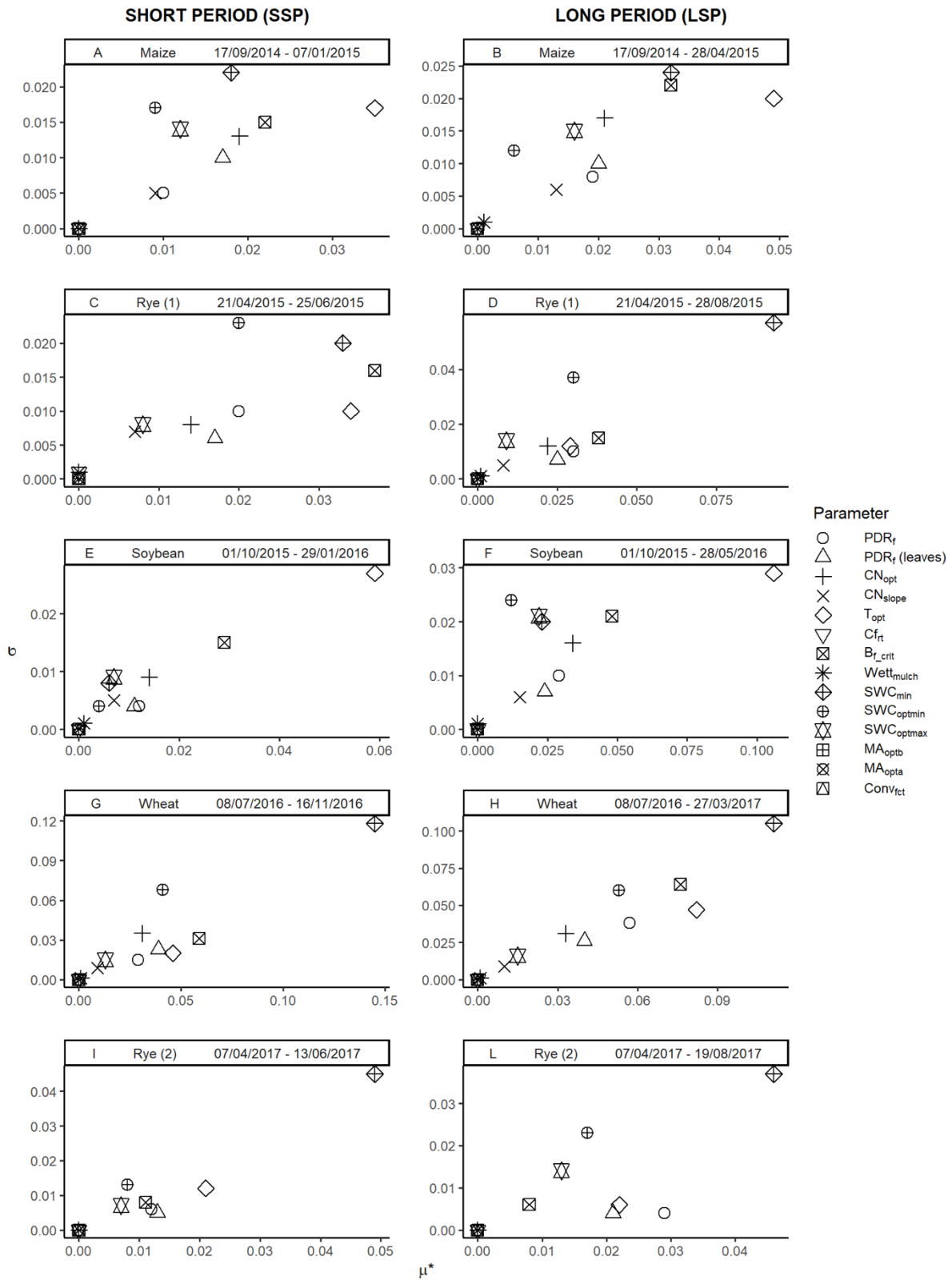


Figure 2. Sensitivity analysis results for the new decomposition module implemented in ARMOSA. Absolute mean ( $\mu^*$ ) and standard deviation ( $\sigma$ ) of elementary effect displayed for each crop and each simulation period (short period, SSP, and long period, LSP).

A valuable indication of the SA results can be retrieved by averaging the Savage-scores (Paleari et al., 2021) of the sensitivity metrics estimated for the different crops and simulation periods (data not shown). The average final ranking allowed us to identify the top parameters associated with surface residue decomposition, regardless of the crop and of the period of decomposition. Starting from the most relevant, the top five parameters were  $T_{opt}$ ,  $SWC_{min}$ ,  $B_{f\_crit}$ ,  $PDR_f$  and  $PDR_f$  (leaves).

Kendall's coefficient of concordance, computed on the whole set of ten SAs, showed a high concordance value ( $C_T = 0.86$ ,  $p\text{-value} < 0.001$ ) meaning that the ten different rankings significantly agreed in the definition of the most important parameters. Table 3 shows the coefficient of concordance and the associated  $p\text{-value}$  among all the SAs. On average, the concordance values within each crop between the short and long period were always high ( $C_T = 98\text{-}99$ , Table 3) and significant ( $p\text{-value} < 0.05$ ). These values reflected the high concordance of the top ranks within every single crop, as shown in Figure 2, even though some differences were found for parameters with lower importance (i.e., lower values of  $\mu^*$ ).

Table 3. Matrix summarizing ten sensitivity analyses (five crops and two simulation periods, the short simulation period, SSP, and the long simulation period, LSP) conducted with the new module implemented into ARMOSA. The top right quadrant reports the coefficients of concordance (Eq. 3, with 10 'raters' and 14 subjects), while the bottom left quadrant reports the associated p-values.

		Coefficient of concordance ( $C_T$ )									
		Maize (SSP)	Maize (LSP)	Rye (1) (SSP)	Rye (1) (LSP)	Soybean (SSP)	Soybean (LSP)	Wheat (SSP)	Wheat (LSP)	Rye (2) (SSP)	Rye (2) (LSP)
$p$ - $v$ $a$   $u$ $e$	Maize (SSP)		0.99	0.95	0.90	0.96	0.98	0.94	0.93	0.86	0.82
	Maize (LSP)	0.019		0.95	0.92	0.96	0.97	0.96	0.96	0.89	0.85
	Rye (1) (SSP)	0.026	0.025		0.98	0.91	0.94	0.98	0.98	0.93	0.9
	Rye (1) (LSP)	0.037	0.031	0.021		0.86	0.89	0.98	0.99	0.92	0.92
	Soybean (SSP)	0.023	0.024	0.034	0.049		0.99	0.88	0.9	0.8	0.77
	Soybean (LSP)	0.019	0.021	0.027	0.04	0.019		0.91	0.92	0.85	0.82
	Wheat (SSP)	0.027	0.024	0.02	0.02	0.042	0.034		0.98	0.92	0.89
	Wheat (LSP)	0.029	0.023	0.019	0.019	0.038	0.031	0.019		0.95	0.93
	Rye (2) (SSP)	0.049	0.041	0.029	0.031	0.076	0.054	0.032	0.026		0.98
	Rye (2) (LSP)	0.068	0.055	0.036	0.033	0.094	0.069	0.041	0.029	0.019	

Based on the season during which the crop residue decomposition occurs (Fig. 1), different crop residues can be compared. Maize residues mostly degraded in the same season as soybean: indeed, the two SA conducted in the two SSP had high concordance ( $C_T = 0.96$ ,  $p\text{-value} = 0.023$ , Table 3), confirming the significant effect of  $T_{opt}$  and  $B_{f\_crit}$ . If we consider the LSP of the same crops, the coefficient of concordance is still significantly

high ( $C_T = 0.97$ ,  $p\text{-value} = 0.024$ , Table 3), emphasizing, again, the importance of the temperature and the critical residue biomass amount (i.e.,  $B_{f\_crit}$ , the critical level of flat residue biomass above which the decomposition is slower) for the surface decomposition process. Wheat residues, differently from the other crop residues, had the longest time of decomposition (262 days of soil covering overall), spanning from late autumn to early summer seasons. For this reason, it did not seem reasonable to compare them with the other crops. The two rye cover crops instead, were terminated almost in the same period, and their residues remained on the soil surface until the end of August. Thus, the coefficients of concordance confirmed the relevance of the soil water content (with  $SWC_{min}$  being the most critical parameter) on the surface decomposition process, even if  $C_T$  was lower compared to those above (for the short simulation periods  $C_T = 0.93$ ,  $p\text{-value} = 0.029$ , while for the long simulation period  $C_T = 0.92$ ,  $p\text{-value} = 0.033$ ). This is mainly due to the second and third positions (alternately belonging to  $T_{opt}$ ,  $B_{f\_crit}$  or  $PDR_f$ ) in the parameter rankings of the two cover crops belonging to different parameters.

#### *The APSIM model*

Compared to ARMOSA, the APSIM model has a lower number of parameters, which cause a lower parameter overlapping in the diagnostic diagrams (Figure 3).

As for maize SA outputs varied between the SSP and LSP. The  $T_{opt}$  parameter clearly had an important role in the surface decomposition process in both simulation periods, but the effect was variable for the other parameters (Fig. 3A/3B). In fact,  $B_{f\_crit}$  played a key role in the SSP, while the potential decomposition rate ( $B_{f\_degr}$ ) assumed a crucial weight for the LSP. All the other parameters (i.e.,  $CN_{opt}$ ,  $CN_{slope}$ ,  $Cf_{rt}$  and  $cum\_eos\_max$ ), even with lower values of  $\sigma$ , also reported lower values of  $\mu^*$ . Thus, they were far away from the top-right quadrant.

For the rye cover crop, the results showed a similar parameters response between SSP and LSP within a single year, but differences emerged when comparing 2015 (i.e., "Rye (1)") to 2017 (i.e., "Rye (2)"). In 2015, the most critical parameter was the  $cum\_eos\_max$ , which scored the highest value in both SSP and LSP (Fig. 3C/3D). In the second and third positions of the ranking, we found the  $B_{f\_degr}$  and  $Cf_{rt}$ , varying between LSP and SSP. All the other parameters have  $\mu^*$  values close to zero, not affecting the SA output.



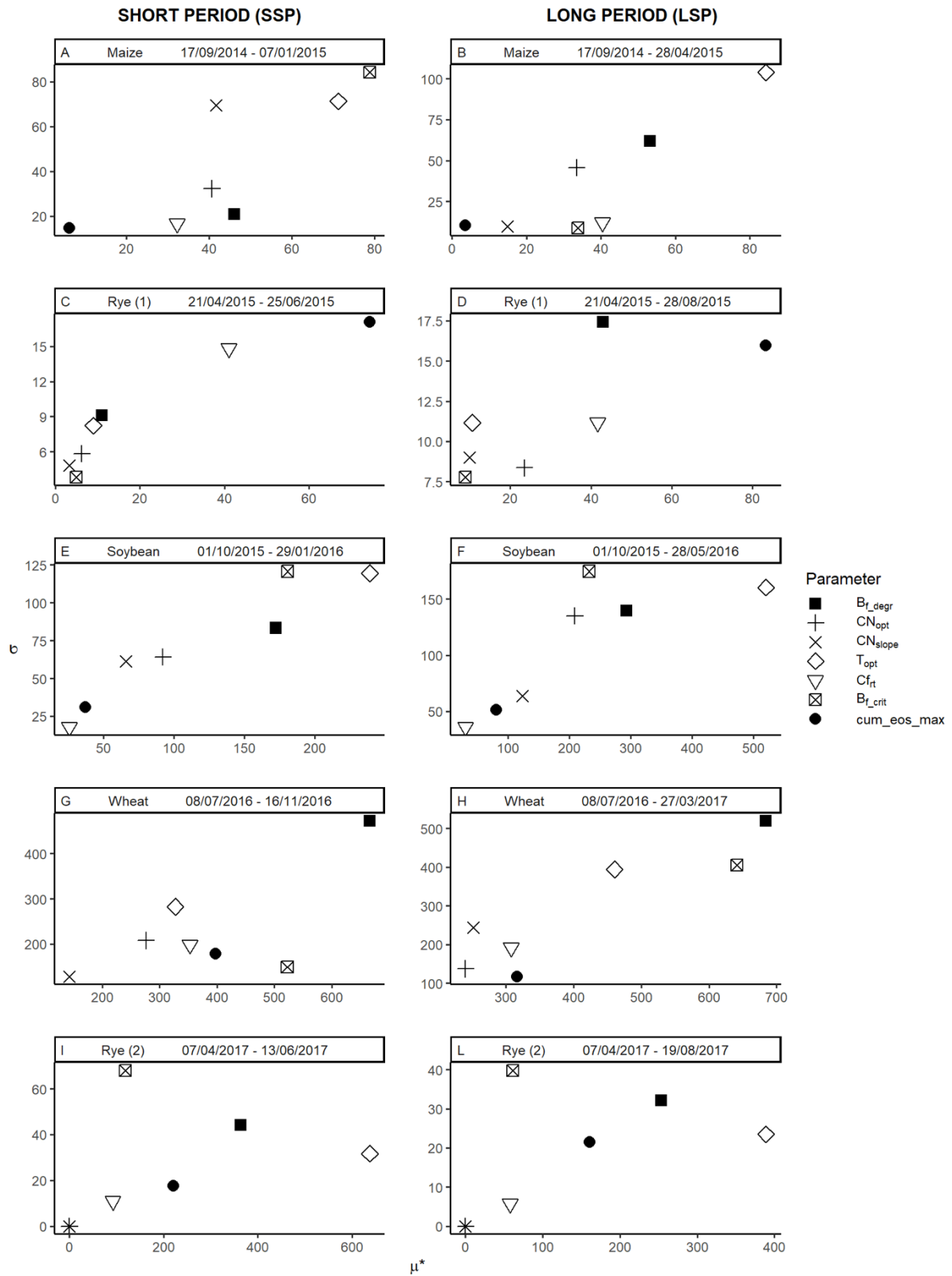


Figure 3. Sensitivity analysis results for the APSIM model. Absolute mean ( $\mu^*$ ) and standard deviation ( $\sigma$ ) of elementary effect displayed for each crop and each simulation period (short period, SSP, and long period, LSP).

In 2017, the most sensitive parameters remained the same as in 2015, but their ranks became considerably different. The temperature had a significant effect on the decomposition process, increasing the weight of the  $T_{opt}$  parameter in the SA analysis (Fig. 3I/3L). The potential decomposition rate ( $B_{f\_degr}$ ) is in the middle of the diagram for both SSP and LSP, always followed by  $cum\_eos\_max$ . Similar results have been observed also in soybean, when  $T_{opt}$  had the most significant impact against all the other parameters (Fig. 3E/3F) in both simulation periods. Focusing on SSP, the SA evidenced  $B_{f\_crit}$  and  $B_{f\_degr}$  as essential parameters affecting the decomposition process, since they are located in the top-right quadrant. In the long period, the weight of  $B_{f\_crit}$  and  $B_{f\_degr}$  is less evident and it is comparable with the weight of  $CN_{opt}$ . In LSP, the clusters of these three last parameters can be easily distinguished for all the other parameters, even though their impact is negligible. Wheat is the only crop heavily influenced by the  $B_{f\_degr}$  parameter, which is constantly at the top right angle of the diagram (Fig. 3G/3H). Nevertheless, the situation becomes different when comparing the SSP with LSP.  $B_{f\_crit}$  had a higher  $\mu^*$  value in LSP, with a high  $\sigma$  value too. In SSP  $B_{f\_crit}$  maintained high  $\mu^*$  value but decreased the interaction with other parameters (lower  $\sigma$  value). In the bottom-left quadrant, the other parameters are less sensitive.  $B_{f\_crit}$  and  $T_{opt}$  had predominant roles in the LSP diagram compared to  $CN_{opt}$ ,  $CN_{slope}$ ,  $C_{rt}$  and  $cum\_eos\_max$  parameters.

Averaging the Savage-scores of the sensitivity metrics, estimated for the different crops and periods, led to an averaged ranking (data not shown). The optimum temperature for decomposition ( $T_{opt}$ ) led the rank, followed by the potential decomposition rate ( $B_{f\_degr}$ ), the critical residue mass ( $B_{f\_crit}$ ) and the cumulative potential soil evaporation ( $cum\_eos\_max$ ).

Kendall's coefficient of concordance computed on the whole set of ten SAs was relatively low ( $C_T = 0.43$ ). The ten different parameter rankings displayed several differences, and therefore are not in agreement between each other in defining the most critical parameters involved in the residue decomposition process, even with a significant test ( $p\text{-value} < 0.001$ ).

Table 4 shows the coefficient of concordance and the associated p-value between all the combinations of SA. In APSIM, within each crop, the concordance values between SSP and LSP were significant ( $P < 0.05$ ) except for maize, and with values almost stable around 90% (Table 4).

Table 4. Matrix summarizing ten sensitivity analyses (five crops and two simulation periods, the short simulation period, SSP, and the long simulation period, LSP) conducted with the APSIM model. The top right quadrant reports the coefficients of concordance (eq. 3, with 10 raters and 7 subjects) while the bottom left quadrant reports the associate p-values.

		Coefficient of concordance ( $C_T$ )									
		Maize (SSP)	Maize (LSP)	Rye (1) (SSP)	Rye (1) (LSP)	Soybean (SSP)	Soybean (LSP)	Wheat (SSP)	Wheat (LSP)	Rye (2) (SSP)	Rye (2) (LSP)
	Maize (SSP)		0.79	0.2	0.14	0.95	0.91	0.61	0.79	0.67	0.67
	Maize (LSP)	0.1		0.54	0.45	0.79	0.82	0.64	0.77	0.79	0.79
	Rye (1) (SSP)	0.935	0.456		0.95	0.29	0.34	0.73	0.61	0.73	0.73
<i>p</i>	Rye (1) (LSP)	0.969	0.615	0.007		0.25	0.34	0.68	0.54	0.64	0.64
<i>v</i>	Soybean (SSP)	0.006	0.092	0.846	0.878		0.98	0.59	0.77	0.75	0.75
<i>a</i>	Soybean (LSP)	0.017	0.069	0.773	0.771	0.002		0.61	0.79	0.79	0.79
<i>l</i>	Wheat (SSP)	0.332	0.272	0.151	0.22	0.35	0.33		0.93	0.79	0.79
<i>u</i>	Wheat (LSP)	0.1	0.117	0.331	0.455	0.116	0.101	0.012		0.9	0.9
<i>e</i>	Rye (2) (SSP)	0.234	0.09	0.144	0.264	0.118	0.087	0.085	0.021		0.98
	Rye (2) (LSP)	0.226	0.09	0.144	0.268	0.118	0.088	0.085	0.019	0.001	

These values reflected the high concordance of the top ranks within every single crop. Based on the season under which the crop residue decomposition occurs (Fig. 1), as already shown with the new module implemented in ARMOSA, different crop residues can be compared to each other. Previously, for the new ARMOSA module, maize results were compared with those of soybean, since the decomposition seasons of these residues were almost the same. The same comparison between maize and soybean was performed with APSIM results: in this case too, the two crop residues led to similar SA outputs. Both the comparisons between SA conducted on the short period (i.e., "Maize (S)" and "Soybean (S)") and long period (i.e., "Maize (L)" and "Soybean (L)") have high coefficients of concordance ( $C_T = 0.95$  and  $C_T = 0.82$ , respectively), even if only the first was significant at the 5% threshold. These coefficients revealed that  $T_{opt}$ ,  $B_{f\_crit}$  and  $B_{f\_degr}$  are the most influent parameters involved in the decomposition process of these crop residue. It is also worth comparing the two cover crops (i.e., "Rye (1)" and "Rye (2)") since their residues decompose in the same season and belong to the same crop species. Nevertheless, for APSIM the concordance coefficients were around 70% but not significant for the short and long period of decomposition ( $p\text{-value} > 0.10$ ).

### 3.4 Discussion

#### 3.4.1 Comparison of modelling approaches based on sensitivity analysis

Performing a set of ten different analyses, based on different crop residues, simulation periods (Table 2) and different seasons during the year (Fig. 1), allowed us to detect the sensitivity of the two models to the main

parameters involved in surface residue decomposition. Moreover, since the SA results change according to the duration of the simulation (i.e., according to the value of the dependent variable at the last time step), the definition of different simulation periods (SSP and LSP) for each crop was useful to better define the parameters' role on residue decomposition kinetics. In fact, considering a single crop at the time and going thought SSP to LSP (i.e., increasing the simulation period), allowed us to detect if some parameters maintained their sensitivity regardless the different conditions.

The variation of parameter sensitivity between the two simulation periods within a single crop was usually lower in the new module (higher coefficients of concordance) than in APSIM, except for the "Rye (1)" crop. In this case, the impact of  $T_{opt}$  and  $B_{f\_crit}$  was higher in SSP than in LSP (Fig. 2C). Probably, before the summer period (July and August 2015), when  $SWC_{min}$  was by far the most relevant parameter, the lower temperature and the initial amount of residues ( $2.85 \text{ Mg ha}^{-1}$ ) have contributed to slow the decomposition in the early stages, thus impacting the SA output. The parameters sensitivity under "Rye (2)" was more homogeneous comparing SSP and LSP. In fact, the temperature during April and May was on average slightly greater compared to 2015 (i.e., not strongly limiting the decomposition) and especially the initial amount of residues ( $2.23 \text{ Mg ha}^{-1}$ ) was closer to the  $B_{f\_crit}$  threshold ( $2.00 \text{ Mg ha}^{-1}$ ).

#### 3.4.2 Temperature, soil water content and residue quantity drive residue decomposition in the new ARMOSA module

Comparing crop residues that decomposed in the same season, the sensitivity analysis of the new module almost ended with the same parameter ranking (as in the case of maize vs soybean or rye (1) vs rye (2)). This is related to the high dependency of surface decomposition on the environmental factors rather than on biomass-specific characteristics (Iqbal et al., 2015; Lee et al., 2014; Marinari et al., 2014; Sanaullah et al., 2012). Even if these specific patterns were found when comparing crop residues having the same season of decomposition, the highly significant coefficients of concordance, for the whole set of ten SAs, highlighted the importance of the top-ranking parameters. Specifically, all the SAs conducted with the new module indicated that  $T_{opt}$  and  $SWC_{min}$  are the most influential parameters, as confirmed by the average ranking. The  $T_{opt}$  parameter, based on soil temperature (that is retrieved in ARMOSA from the simulated temperature of the 5 cm topsoil layer), reflects the optimum temperature for the activity of the microbial community that is

primarily involved in residue decomposition (Findeling et al., 2007), whose importance is well recognized (Findeling et al., 2007; Nicolardot et al., 2001) and gives the temperature a crucial role in the simulations.

When the temperature is not the limiting factor, the  $SWC_{min}$  became the most influential parameter, confirming that moisture limitation is also essential in this process (Coppens et al., 2007), especially if the residues are left on the soil surface (Lee et al., 2014).  $SWC_{min}$  is related to soil water retention; it defines the minimum residue water content for decomposition, expressed as a proportion of field water capacity. As expected, this parameter limited the decomposition mainly for crop residues laying on the soil surface during the dry period, such as in spring (in rye) or, even partially, in summer (in wheat). During the autumn/winter period, when soil water content is not limiting anymore, the importance of this parameter became lower (in maize) or even roughly negligible (in soybean). In the new module approach,  $SWC_{min}$  is used in the moisture factor equation (Eq. 10, Appendix A), representing the influence of soil water content on flat residue wetness and, consequently, on their decomposition rate. In ARMOSA, this parameter is based on the soil water content, while other modelling approaches are based on the biomass water content (Findeling et al., 2007). Even if the biomass water content rather than the soil water content is in principle more adequate, the soil water content of the top layer appears to be a good "proxy" of surface residue water content. In fact, the mass adjacent to the soil tends to adsorb water and to be rewetted by the underneath soil layer (Iqbal et al., 2015) in a phenomenon defined "sponge effect" (Kravchenko et al., 2017).

The role of the  $B_{f\_crit}$  parameter (i.e., the critical flat residue biomass above which the decomposition is slower) in the new module is worth mentioning: eight out of ten SAs included it in the list of the first three most influencing parameters. Even though  $B_{f\_crit}$  is not explicitly related to the crop biomass properties, it is linked to the specific crop management. For example, in the cases of maize and wheat, the high amount of surface residues found after the harvest is a direct consequence of a farmer management choice. This parameter indirectly reflects the thickness of surface residue biomass, suggesting that the more residue biomass, the slower the decomposition process. Its importance was already reported by Thorburn et al. (2001) who stated that the "upper" mulch layer (i.e., the layer that is not in contact with the soil) has a negligible decomposition rate. The response of the model to this situation (i.e., when crop residue biomass is greater than  $2 \text{ Mg ha}^{-1}$ , Table 1,  $B_{f\_crit}$ ) is essential to avoid early overestimation of the carbon and nitrogen

accumulation in soil due to the whole residue decomposition after a harvest/termination event (Fang et al., 2019). Further model improvements may consider recent findings that demonstrated that the upper mulch layer slowly decomposes and that there is a gradient of moisture and decomposition rate (Dietrich et al., 2019).

We concluded that for the new module application within ARMOSA model framework, an accurate estimation of  $T_{opt}$ ,  $SWC_{min}$  and  $B_{f\_crit}$  is needed to properly simulate the residue decomposition.

On the other hand, it seems also reasonable to include the two potential decomposition rates ( $PDR_f$  and  $PDR_f$  (leaves)) within the set of most influential parameters. Nevertheless, even if  $\mu^*$  for these parameters was never null, they never appeared in the most critical top-right quadrant (Fig. 2). For the new module, this is probably due to the large impact of the environmental factors on decomposition, as indicated by  $T_{opt}$  and  $SWC_{min}$ . In addition, the fact that different  $PDR_f$  and  $PDR_f$  (leaves) values were assigned to each crop (Table 1) did not overestimate or underestimate the maximum rate of residue decomposition (i.e., making the parameters impacting more on the SA), leaving the other parameters to drive this process.

#### 3.4.3 Temperature and potential decomposition rate drive residue decomposition in APSIM

In APSIM, the SA concordance between short and long simulation periods within each crop was lower than in the new module. In other words, the APSIM parameter reacted more to the simulation period increment regardless the crop residues considered. This is evident by observing the SA results of maize ( $C_T = 0.79$ ,  $p$ -value = 0.1, Table 4) and wheat ( $C_T = 0.93$ ,  $p$ -value = 0.012, Table 4) showed in figure 3. In the case of maize, the initial amount of residues ( $11.7 \text{ Mg ha}^{-1}$ ) probably had a more considerable impact on the SSP SA output compared to the analysis "spreaded" between 17/09/2014 and 28/04/2015 (LSP). This is confirmed by the mathematical implementation shared with ARMOSA and reported in Eq. 13 (Appendix A): when  $B_f > B_{f\_crit}$ , then the decomposition is reduced exponentially. Moving away from the harvest date (i.e., increasing the duration of the decomposition), the  $B_{f\_crit}$  lost its importance (as already noted with rye (1) with the new module), favoring the temperature (through  $T_{opt}$ ) and the potential decomposition rate ( $B_{f\_degr}$ ) limitations (Fig. 3B). In the case of wheat instead (Fig. 3G/3H), the role of  $B_{f\_crit}$ , together with  $T_{opt}$ , became higher in the long compared to the short period. This is probably due to the inclusion of the winter season in the long period, that decreased the  $B_{f\_degr}$  impact compared to the other parameters. In other words, when

temperature does not limit decomposition (as it frequently happens during the short period for wheat), the potential decomposition rate ( $B_{f\_degr}$ ) is the parameter that limit the process the most. Conversely, in the long period most of the decomposition occurs during the coldest months of the year, therefore the temperature interacts more with other parameters (higher value of  $\sigma$ , Fig. 3H), as showed in this case with  $B_{f\_crit}$ .

Looking at the general trends found in APSIM, the impact of the different parameters partially reflected what was found in the new module implemented in ARMOSA. We found  $T_{opt}$  and  $B_{f\_degr}$  in the first two ranking positions in almost all APSIM's SAs. Most of the SAs confirmed the high weight of these parameters except for the rye cover crop in 2015 ("Rye (1)", Fig. 3C/3D). This behavior in 2015 probably reflects the low water availability during summer (180 mm of rainfall between 21/04/2015 and 28/08/2015) limiting surface decomposition (through the *cum\_eos\_max* parameter) more than other factors. Thus, except for this specific situation, the only parameter related to water availability (*cum\_eos\_max*) did not influence the output as  $SWC_{min}$  did with the new module. The APSIM moisture factor considers the water availability using the cumulative potential soil evaporation (and thus the critical cumulative evaporation, *cum\_eos\_max*) to depict the effect that dry residues decompose more slowly than wet residues (Dietrich et al., 2019). Therefore, in this case, a soil property has been used as a proxy for surface residue moisture.

Contrary to the new module, the APSIM potential decomposition rate ( $B_{f\_degr}$ ) significantly impacted the SA output compared to the other parameters involved. The assumption of a unique default value for the decomposition rate ( $B_{f\_degr} = 0.1 \text{ kg m}^{-2} \text{ day}^{-1}$ ) in the APSIM model undoubtedly impacted the SA results more than the crop-specific rates employed in the new ARMOSA module. Specific calibration of this parameter is necessary to properly calibrate the model.

Another similarity in the behavior of the two approaches concerns the importance of  $B_{f\_crit}$ . This parameter is taken from the APSIM equation that limits the decomposition based on the residue amount on the soil surface. Sharing the same equation, the two models gave comparable weight to the limitation of the decomposition rate above a  $2 \text{ Mg ha}^{-1}$  residue biomass threshold, confirming that the models responded in the same way to the amount of crop residue.

### 3.4.5 Evaluation of model plasticity

As a general trend, the two approaches gave comparable results for crop residue that share the same season of decomposition, highlighting the impact of environmental conditions. This agrees with Francos et al. (2003) and Richter et al. (2010), who stated that sensitivity analysis refers to specific conditions and it is not a general property of a model. At least for the new module, the high value of the concordance coefficient, computed on the whole set of SAs, highlighted that some parameters are the most important regardless the specific conditions of the crop biomass.

To better understand the model's behavior, the plasticity index (" $L$ ") has been computed on the whole set of SAs according to Confalonieri et al. (2012). This index (that ranges between 0 and 1, with the highest plasticity at 0) defines the tendency of the model to change its behavior under different conditions. This index has to be intended only to compare models since specific minimum or maximum optimal plasticity values have not been defined. The low value obtained for APSIM ( $L = 0.14$ ) describes a model with higher plasticity compared to the new module ( $L = 0.27$ ). In other words, APSIM has more capability to react to an environmental change by altering the importance of its parameters (confirming the lower value of concordance coefficients). In the discussion above we highlighted that, in the new module, the  $T_{opt}$  and  $SWC_{min}$  had always a great impact on the SAs, probably leading to a lower plasticity compared to APSIM. Nevertheless, situations like rye (1) or wheat (comparing SSP and LSP in Fig. 2) still defined a module capable to change its parameters sensitivity to the environmental changes.

## 3.5 Conclusions

With this work a new module has been developed to explicitly include surface residue pools in many relevant modelling processes. In fact, the implementation of this new module into ARMOSA allowed to simulate many processes in which crop residues, laying on the soil surface, play a crucial role in water and nutrient cycling dynamics. Despite previous implementation of the surface residue decomposition, we developed a new module that simulates this process including all the important factors that give a complete representation of residue decomposition.

The APSIM model was used as a benchmark. This model was selected for its algorithm affinity to ARMOSA and for being a cropping system model widely cited in the literature.



A sensitivity analysis was conducted for each crop residue under analysis (i.e., maize, rye, soybean and wheat). In the present SA we distinguished between long and short simulation periods with the advantage of recognizing if some parameters, within single crop, impacted on the decomposition process regardless the different environmental conditions.

The most important parameters in the new module reflected the importance of the soil temperature ( $T_{opt}$ ), the soil water content ( $SWC_{min}$ ), and the residue biomass ( $B_{f\_crit}$ ) on the decomposition process. The two decomposition rates (PDR<sub>f</sub> and PDR<sub>f</sub> (leaves)) had minor importance, highlighting that, when setting crop specific values, other environment-related parameters are more relevant for the actual decomposition rate. The APSIM model, showed a lower concordance of SA results passing from a crop residue to another and even when comparing short and long simulation periods within the same crop. For maize and wheat, the SA output showed how the duration of the decomposition along different seasons could heavily influence the parameters impact. As a general trend, we always found  $T_{opt}$  and  $B_{f\_degr}$  parameters in the first two rank positions. In addition, having assumed a unique default value for the decomposition rate,  $B_{f\_degr}$  could have impacted the surface residue destiny more than the new module decomposition rates.

The outcome of this work allowed us to identify the most relevant parameters for a future work of the model calibration and to evaluate its behavior under variable conditions of the residue surface decomposition process.

### [Acknowledgments](#)

This work was carried out under the project “Innovazioni per estendere l’uso delle colture di copertura in Lombardia - Innovations to extend the use of cover crops in Lombardy”, funded by the Rural Development Programme 2014-2020 of Regione Lombardia, Italy, Operation 16.1.01 (EIP-AGRI Operational Groups).

This study is also funded by the European Union’s Horizon 2020 Framework Programme for Research and Innovation (H2020-RUR-2017-2) as part of the LANDSUPPORT project (grant agreement No. 774234), which aims at developing a decision support system for optimizing soil management in Europe.

### [Sample Credit author statement](#)

**Tommaso Tadiello:** Conceptualization, Software, Methodology, Formal Analysis, Investigation, Writing - Original draft, **Mara Gabbrielli:** Methodology, Software, Investigation, Writing - Original draft, **Marco Botta:** Methodology, Software, Writing- Reviewing and Editing, **Marco Acutis:** Conceptualization, Supervision,

Writing- Reviewing and Editing, **Luca Bechini**: Conceptualization, Supervision, Writing- Reviewing and Editing, Funding acquisition, **Giorgio Ragagnini**: Conceptualization, Writing- Reviewing and Editing, **Andre Fiorini**: Resources, Conceptualization, Writing- Reviewing and Editing, **Vincenzo Tabaglio**: Resources, Conceptualization, Writing- Reviewing and Editing, **Alessia Perego**: Conceptualization, Writing- Reviewing and Editing, Supervision, Project administration, Funding acquisition.

## References

- Alberts, E. E., Holzhey, C. S., West L. T., Nordin, J. O, 1987. Soil Selection: USDA water erosion prediction project (WEPP). Paper No. 87-2542, Am. Soc. Agric. Eng., St. Joseph, MI.
- Biavetti, I., Karetos, S., Ceglar, A., Toreti, A., Panagos, P., 2014. European meteorological data: contribution to research, development, and policy support, in: Hadjimitsis, D.G., Themistocleous, K., Michaelides, S., Papadavid, G. (Eds.). Presented at the Second International Conference on Remote Sensing and Geoinformation of the Environment (RSCy2014), Paphos, Cyprus, p. 922907. <https://doi.org/10.1117/12.2066286>.
- Boselli, R., Fiorini, A., Santelli, S., Ardenti, F., Capra, F., Maris, S.C., Tabaglio, V., 2020. Cover crops during transition to no-till maintain yield and enhance soil fertility in intensive agro-ecosystems. *Field Crops Research* 255, 107871. <https://doi.org/10.1016/j.fcr.2020.107871>.
- Brisson, N., Itier, B., L'Hotel, J.C., Lorendeau, J.Y., 1998. Parameterisation of the Shuttleworth-Wallace model to estimate daily maximum transpiration for use in crop models. *Ecological Modelling* 107, 159–169. [https://doi.org/10.1016/S0304-3800\(97\)00215-9](https://doi.org/10.1016/S0304-3800(97)00215-9).
- Bruun, S., Luxhoi, J., Magid, J., Deneergaard, A., Jensen, L., 2006. A nitrogen mineralization model based on relationships for gross mineralization and immobilization. *Soil Biology and Biochemistry* 38, 2712–2721. <https://doi.org/10.1016/j.soilbio.2006.04.023>.
- Campolongo, F., Cariboni, J., Saltelli, A., 2007. An effective screening design for sensitivity analysis of large models. *Environmental Modelling & Software* 22, 1509–1518. <https://doi.org/10.1016/j.envsoft.2006.10.004>.
- Campolongo, F., Carboni, J., Saltelli, A., Schoutens, W., 2004. Enhancing the Morris method. In: Hanson, K.M., Hemez, F.M. (Eds.), *Proceedings of the 4th International Conference on Sensitivity Analysis of Model Output*. Santa Fe, New Mexico, March 8–11, pp. 369–379.
- Chaves, B., Redin, M., Giacomini, S.J., Schmatz, R., Léonard, J., Ferchaud, F., Recous, S., 2021. The combination of residue quality, residue placement and soil mineral N content drives C and N dynamics by modifying N availability to microbial decomposers. *Soil Biology and Biochemistry* 163, 108434. <https://doi.org/10.1016/j.soilbio.2021.108434>.
- Confalonieri, R., Bregaglio, S., Acutis, M., 2012. Quantifying plasticity in simulation models. *Ecological Modelling* 225, 159–166. <https://doi.org/10.1016/j.ecolmodel.2011.11.022>.
- Confalonieri, R., Acutis, M., Bellocchi, G., Cerrani, I., Tarantola, S., Donatelli, M., Genovese, G., 2006. Exploratory sensitivity analysis of cropsyst, warm and wofost: a case-study with rice biomass simulations. *Italian Journal of Agrometeorology* 17 - 25 (3).
- Coppens, F., Garnier, P., Findeling, A., Merckx, R., Recous, S., 2007. Decomposition of mulched versus incorporated crop residues: Modelling with PASTIS clarifies interactions between residue quality and location. *Soil Biology and Biochemistry* 39, 2339–2350. <https://doi.org/10.1016/j.soilbio.2007.04.005>.
- Diel, J., Franko, U., 2020. Sensitivity analysis of agricultural inputs for large-scale soil organic matter modelling. *Geoderma* 363, 114172. <https://doi.org/10.1016/j.geoderma.2020.114172>.
- Dietrich, G., Recous, S., Pinheiro, P.L., Weiler, D.A., Schu, A.L., Rambo, M.R.L., Giacomini, S.J., 2019. Gradient of decomposition in sugarcane mulches of various thicknesses. *Soil and Tillage Research* 192, 66–75. <https://doi.org/10.1016/j.still.2019.04.022>.

- Dietrich, G., Sauvadet, M., Recous, S., Redin, M., Pfeifer, I.C., Garlet, C.M., Bazzo, H., Giacomini, S.J., 2017. Sugarcane mulch C and N dynamics during decomposition under different rates of trash removal. *Agriculture, Ecosystems & Environment* 243, 123–131. <https://doi.org/10.1016/j.agee.2017.04.013>.
- Douglas, C.L., Allmaras, R.R., Rasmussen, P.E., Ramig, R.E., Roager, N.C., 1980. Wheat straw composition and placement effects on decomposition in dryland agriculture of the Pacific Northwest. *Soil Science Society of America Journal* 44, 833–837. <https://doi.org/10.2136/sssaj1980.03615995004400040035x>.
- Fang, Y., Singh, B.P., Cowie, A., Wang, W., Arachchi, M.H., Wang, H., Tavakkoli, E., 2019. Balancing nutrient stoichiometry facilitates the fate of wheat residue-carbon in physically defined soil organic matter fractions. *Geoderma* 354, 113883. <https://doi.org/10.1016/j.geoderma.2019.113883>.
- FAO, 2016. Save and Grow in practice: Maize, rice and wheat. Rome. <https://www.fao.org/3/i4009e/i4009e.pdf>.
- Findeling, A., Garnier, P., Coppens, F., Lafolie, F., Recous, S., 2007. Modelling water, carbon and nitrogen dynamics in soil covered with decomposing mulch. *Eur J Soil Science* 58, 196–206. <https://doi.org/10.1111/j.1365-2389.2006.00826.x>.
- Fiorini, A., Boselli, R., Maris, S. C., Santelli, S., Perego, A., Acutis, M., ... & Tabaglio, V. (2020). Soil type and cropping system as drivers of soil quality indicators response to no-till: A 7-year field study. *Applied Soil Ecology*, 155, 103646. <https://doi.org/10.1016/j.apsoil.2020.103646>.
- Francos, A., Elorza, F.J., Bouraoui, F., Bidoglio, G., Galbiati, L., 2003. Sensitivity analysis of distributed environmental simulation models: understanding the model behaviour in hydrological studies at the catchment scale. *Reliability Engineering & System Safety* 79, 205–218. [https://doi.org/10.1016/S0951-8320\(02\)00231-4](https://doi.org/10.1016/S0951-8320(02)00231-4).
- Guérif, J., Richard, G., Durr, C., Machet, J.M., Recous, S., Roger- Estrade, J., 2001. A review of tillage effects on crop residue management, seedbed conditions and seedling establishment. *Soil and Tillage Research* 61, 13–32. [https://doi.org/10.1016/S0167-1987\(01\)00187-8](https://doi.org/10.1016/S0167-1987(01)00187-8).
- Herman, J. and Usher, W., 2017. SALib: An open-source Python library for sensitivity analysis. *Journal of Open Source Software*, 2(9). Doi:10.21105/joss.00097.
- Holzworth, D.P., Huth, N.I., deVoil, P.G., Zurcher, E.J., Herrmann, N.I., McLean, G., Chenu, K., van Oosterom, E.J., Snow, V., Murphy, C., Moore, A.D., Brown, H., Whish, J.P.M., Verrall, S., Fainges, J., Bell, L.W., Peake, A.S., Poulton, P.L., Hochman, Z., Thorburn, P.J., Gaydon, D.S., Dalgliesh, N.P., Rodriguez, D., Cox, H., Chapman, S., Doherty, A., Teixeira, E., Sharp, J., Cichota, R., Vogeler, I., Li, F.Y., Wang, E., Hammer, G.L., Robertson, M.J., Dimes, J.P., Whitbread, A.M., Hunt, J., van Rees, H., McClelland, T., Carberry, P.S., Hargreaves, J.N.G., MacLeod, N., McDonald, C., Harsdorf, J., Wedgwood, S., Keating, B.A., 2014. APSIM – evolution towards a new generation of agricultural systems simulation. *Environ. Model. Softw.* 62, 327–350. <https://doi.org/10.1016/j.envsoft.2014.07.009>.
- Iman, R. L., and W. J. Conover. "A Measure of Top-Down Correlation." *Technometrics*, vol. 29, no. 3, 1987, pp. 351–57, <https://doi.org/10.2307/1269344>. Accessed 5 Apr. 2022.
- Iooss, B., Da Veiga, S., Janon, A., and Gilles Pujol, 2021. sensitivity: Global Sensitivity Analysis of Model Outputs, <https://CRAN.R-project.org/package=sensitivity> to link to this page (version 1.27.0).
- Iqbal, A., Aslam, S., Alavoine, G., Benoit, P., Garnier, P., Recous, S., 2015. Rain regime and soil type affect the C and N dynamics in soil columns that are covered with mixed-species mulches. *Plant Soil* 393, 319–334. <https://doi.org/10.1007/s11104-015-2501-x>.
- Izaurralde, R.C., Williams, J.R., McGill, W.B., Rosenberg, N.J., Jakas, M.C.Q., 2006. Simulating soil C dynamics with EPIC: Model description and testing against long-term data. *Ecological Modelling* 192, 362–384. <https://doi.org/10.1016/j.ecolmodel.2005.07.010>.
- Justes, E., Mary, B. & Nicolardot, B. Quantifying and modelling C and N mineralization kinetics of catch crop residues in soil: parameterization of the residue decomposition module of STICS model for mature and non mature residues. *Plant Soil* 325, 171–185 (2009). <https://doi.org/10.1007/s11104-009-9966-4>.

- Kravchenko, A.N., Toosi, E.R., Guber, A.K., Ostrom, N.E., Yu, J., Azeem, K., Rivers, M.L., Robertson, G.P., 2017. Hotspots of soil N<sub>2</sub>O emission enhanced through water absorption by plant residue. *Nature Geosci* 10, 496–500. <https://doi.org/10.1038/ngeo2963>.
- Lee H., Fitzgerald J., Hewins D.B., McCulley R.L., Archer S.R., Rahn T., Throop H.L., 2014. Soil moisture and soil-litter mixing effects on surface litter decomposition: a controlled environment assessment. *Soil Biol Biochem* 72:123–132. <https://doi.org/10.1016/j.soilbio.2014.01.027>.
- Legendre, P., 2005. Species associations: the Kendall coefficient of concordance revisited. *JABES* 10, 226–245. <https://doi.org/10.1198/108571105X46642>.
- Meier, E.A., Thorburn, P.J., 2016. Long Term Sugarcane Crop Residue Retention Offers Limited Potential to Reduce Nitrogen Fertilizer Rates in Australian Wet Tropical Environments. *Front. Plant Sci.* 7. <https://doi.org/10.3389/fpls.2016.01017>.
- Marinari, S., Mancinelli, R., Brunetti, P., Campiglia, E., 2015. Soil quality, microbial functions and tomato yield under cover crop mulching in the Mediterranean environment. *Soil and Tillage Research* 145, 20–28. <https://doi.org/10.1016/j.still.2014.08.002>.
- Miguez, F., 2022. *apsimx: Inspect, Read, Edit and Run 'APSIM' "Next Generation" and 'APSIM' Classic.* <https://CRAN.R-project.org/package=apsimx> (version 2.3.1).
- Moreno-Cornejo, J., Zornoza, R., Faz, A., 2014. Carbon and nitrogen mineralization during decomposition of crop residues in a calcareous soil. *Geoderma* 230–231, 58–63. <https://doi.org/10.1016/j.geoderma.2014.03.024>.
- Morris, M.D., 1991. Factorial sampling plans for preliminary computational experiments. *Technometrics* 33, 161–174.
- Nicolardot, B., Recous, S. & Mary, B. Simulation of C and N mineralisation during crop residue decomposition: A simple dynamic model based on the C:N ratio of the residues. *Plant and Soil* 228, 83–103 (2001). <https://doi.org/10.1023/A:1004813801728>.
- Paleari, L., Movedi, E., Zoli, M., Burato, A., Cecconi, I., Errahouly, J., Pecollo, E., Sorvillo, C., Confalonieri, R., 2021. Sensitivity analysis using Morris: Just screening or an effective ranking method? *Ecological Modelling* 455, 109648. <https://doi.org/10.1016/j.ecolmodel.2021.109648>.
- Perego, A., Giussani, A., Sanna, M., Fumagalli, M., Carozzi, M., Alfieri, L., Brenna, S., Acutis, M., 2013. The ARMOSA simulation crop model: overall features, calibration and validation results. *Italian Journal of Agrometeorology* 3, 23–38.
- Pianosi, F., Beven, K., Freer, J., Hall, J.W., Rougier, J., Stephenson, D.B., Wagener, T., 2016. Sensitivity analysis of environmental models: a systematic review with practical workflow. *Environ. Model. Softw.* 79, 214–232. <https://doi.org/10.1016/j.envsoft.2016.02.008>.
- Probert, M.E., Dimes, J.P., Keating, B.A., Dalal, R.C., Strong, W.M., 1998. APSIM's water and nitrogen modules and simulation of the dynamics of water and nitrogen in fallow systems. *Agricultural Systems* 56, 1–28. [https://doi.org/10.1016/S0308-521X\(97\)00028-0](https://doi.org/10.1016/S0308-521X(97)00028-0).
- Richter, G.M., Acutis, M., Trevisiol, P., Latiri, K., Confalonieri, R., 2010. Sensitivity analysis for a complex crop model applied to Durum wheat in the Mediterranean. *European Journal of Agronomy* 32, 127–136. <https://doi.org/10.1016/j.eja.2009.09.002>.
- Robertson, F.A., Armstrong, R., Partington, D., Perris, R., Oliver, I., Aumann, C., Crawford, D., Rees, D., 2015. Effect of cropping practices on soil organic carbon: evidence from long-term field experiments in Victoria, Australia. *Soil Research* 53, 636–646. <https://doi.org/10.1071/SR14227>.
- Rumpel, C., 2011. Carbon storage and organic matter dynamics in grassland soils. in: Lemaire, G., Hodgson, J., Chabbi, A. (eds). *Grassland productivity and ecosystem services*. CAB International, Wallingford, U.K., pp 65–72.
- Saltelli, A., Ratto, M., Andres, T., Campolongo, F., Cariboni, J., Gatelli, D., Saisana, M., Tarantola, S., 2007. *Global Sensitivity Analysis. The Primer*. John Wiley & Sons Ltd, Chichester, UK.
- Saltelli, A., Tarantola, S., Campolongo, F., Ratto, M., 2004. *Sensitivity analysis in practice*. Wiley, New York.

- Sanaullah, M., Rumpel, C., Charrier, X., Chabbi, A., 2012. How does drought stress influence the decomposition of plant litter with contrasting quality in a grassland ecosystem? *Plant Soil* 352, 277–288. <https://doi.org/10.1007/s11104-011-0995-4>.
- Savage, R., 1954. Contributions to the theory of rank order statistics - The two-sample case *The Annals of Mathematical Statistics*.
- Scopel, E., B. Muller, J.M. Arreola Tostado, E. Chavez Guerra and F. Maraux. 1998. Quantifying and modeling the effects of light crop residue mulch on water balance: An application to rain-fed maize in western Mexico. Paper presented at the 16th International Congress of Soil Science, Montpellier, France, Aug. 20-26, 1998.
- Soil Survey Staff, 2014. Key to Soil Taxonomy, 12th Edition. Natural Resources Conservation Service of the United States Department of Agriculture, Washington, DC, USA.
- Stella, T., Mouratiadou, I., Gaiser, T., Berg-Mohnicke, M., Wallor, E., Ewert, F., Nendel, C., 2019. Estimating the contribution of crop residues to soil organic carbon conservation. *Environ. Res. Lett.* 14, 094008. <https://doi.org/10.1088/1748-9326/ab395c>.
- Stott, H.F., Stroo, H.F., Elliot, L.F., Papendick, R.I., Unger, P.W., 1990. Wheat residue loss from fields under no-till management. *Soil Sci. Soc. Am. J.* 54, 92±98.
- Tarik C. G., 2019. synchrony: Methods for Computing Spatial, Temporal, and Spatiotemporal Statistics. <http://github.com/tgouhier/synchrony> (version 0.3.8).
- Thorburn, P.J., Probert, M.E., Robertson, F.A., 2001. Modelling decomposition of sugar cane surface residues with APSIM–Residue. *Field Crops Research* 70, 223–232. [https://doi.org/10.1016/S0378-4290\(01\)00141-1](https://doi.org/10.1016/S0378-4290(01)00141-1).
- Valkama, E., Kunyapiyeva, G., Zhapayev, R., Karabayev, M., Zhusupbekov, E., Perego, A., Schillaci, C., Sacco, D., Moretti, B., Grignani, C., Acutis, M., 2020. Can conservation agriculture increase soil carbon sequestration? A modelling approach. *Geoderma* 369, 114298. <https://doi.org/10.1016/j.geoderma.2020.114298>.
- Williams, J.R., Jones, C.A., Dyke, P.T., 1984. A modeling approach to determining the relationship between erosion and soil productivity. *Trans. ASAE* 27, 129–144.

## Appendix A

The module divides surface residues in a standing ( $B_s$ , kg DM m<sup>-2</sup>) and a flat ( $B_f$ , kg DM m<sup>-2</sup>) component. The flat component is further divided in two pools (stem and leaves) to better represent the specific characteristics of the plant fractions (in terms of C:N ratio and potential decomposition rate). Numerical integration is performed to calculate the values of  $B_s$  and  $B_f$  at each time step (Eq. 1 and 2).

$$B_{s(t)} = B_{s(t-1)} - dB_{s\_degr} + dB_{s\_part} - dB_{s\_conv} - dB_{s\_till} \quad [1]$$

$$B_{f(t)} = B_{f(t-1)} - dB_{f\_degr} + dB_{f\_part} + dB_{s\_conv} - dB_{f\_till} \quad [2]$$

The processes represented by the module rates are the following: residue decomposition ( $dB_{s\_degr}$  and  $dB_{f\_degr}$ , kg DM m<sup>-2</sup> d<sup>-1</sup>), residue partitioning at harvest ( $dB_{s\_part}$  and  $dB_{f\_degr}$ , kg DM m<sup>-2</sup> d<sup>-1</sup>), standing residue conversion into flat residue ( $dB_{s\_conv}$ , kg DM m<sup>-2</sup> d<sup>-1</sup>) and residue incorporation into soil through tillage operation ( $dB_{s\_till}$  and  $dB_{f\_till}$ , kg DM m<sup>-2</sup> d<sup>-1</sup>).

Partitioning of the surface residue ( $B_{tot}$ , kg DM m<sup>-2</sup>) in  $B_s$  and  $B_f$  is simulated using WEPP approach. The partitioning is estimated at harvest, before any other management operation, using the ratio between the cutting height ( $H_{cut}$ , m) and the crop height ( $H_{cm}$ , m) to determine the portion ( $F_{pc}$ , unitless, Eq. 3) of initial residue that becomes standing residue (Eq. 4). The portion of flat residue (Eq. 5) is determined as a complement ( $1-F_{pc}$ ).

$$F_{pc} = \frac{H_{cut}}{H_{cm}} \quad [3]$$

$$dB_{s\_part} = B_{tot}F_{pc} \quad [4]$$

$$dB_{f\_part} = B_{tot}(1 - F_{pc}) \quad [5]$$

The decomposition of the standing residue ( $dB_{s\_degr}$ , kg DM m<sup>-2</sup> d<sup>-1</sup>, Eq. 6) is also simulated adopting WEPP approach (Eq. 6).

$$dB_{s\_degr} = B_{s(t-1)}e^{-PDR_{stand}fD_{stand}Size_iFert_i} \quad [6]$$

The amount of remaining standing residue biomass at the end of the simulated time step depends on three limiting factors ( $fD_{stand}$ ,  $Size_i$  and  $Fert_i$ ) that affect the optimal decomposition rate ( $PDR_{stand}$ , kg m<sup>-2</sup> d<sup>-1</sup>) of a specific residue type.  $fD_{stand}$ ,  $Size_i$  and  $Fert_i$  consider respectively the limitations due to environment conditions, soil fertility and residue size.

The limiting factor that represents the environmental limitations that condition standing residue decomposition in field ( $fD_{stand}$ , unitless) considers the residue water content and the air temperature as independent limiting factors. The water limiting factor ( $fW_{stand}$ , unitless, Eq. 7) is obtained as the ratio between the rainfall of the considered time step ( $Rain$ , m) and a parameter representing the amount of rain that saturates the standing residue ( $Rain_{sat}$ , m) whose default value is 0.004. The limiting factor ranges between 0 and 1 depending on the standing residue water content and on daily average temperature ( $T_{avg}$ , °C).

$$fW_{stand} = \begin{cases} \frac{Rain}{Rain_{sat}} & \text{if } PRCP \leq Rain_{sat} \\ 1 & \text{if } PRCP > Rain_{sat} \\ 0 & \text{if } T_{avg} < 0 \end{cases} \quad [7]$$

The temperature limiting factor ( $fT_{stand}$ , unitless, Eq. 8) ranges between 0 and 1, and it is calculated as a function of daily average temperature ( $T_{avg}$ , °C) designed for temperate regions and defined by two parameters: the maximum ( $T_{max}$ , °C) and the minimum ( $T_{min}$ , °C) temperature for microbial decomposition of residues. This function is limited also by the temperature above which the microbial activity stops ( $T_{lim}$ , °C).

$$fT_{stand} = \begin{cases} \frac{2(T_{avg}+T_{min})^2(T_{max}+T_{min})^2-(T_{avg}+T_{min})^4}{(T_{max}+T_{min})^4} \\ 0 & \text{if } T_{avg} < T_{min} \text{ or } T_{avg} > T_{lim} \end{cases} \quad [8]$$

The decomposition of flat residue biomass ( $dB_{f\_degr}$ , kg DM m<sup>-2</sup> d<sup>-1</sup>) is simulated adopting APSIM approach that estimates the fraction of decayed biomass for each time step (Eq. 9). This approach is similar to the one adopted for the standing residue (WEPP model) but employs additional limiting factors. The decomposition rate is described as a function of: an optimal decomposition rate ( $PDR_{flat}$ , kg m<sup>-2</sup> d<sup>-1</sup>), environmental limiting factor such as a temperature ( $fT_{flat}$ , unitless) and a soil moisture ( $fW_{flat}$ , unitless) factor, and residue dependent limiting factors such as the C:N ratio ( $fCN_{flat}$ , unitless) and soil-residue contact degree ( $fContact_{flat}$ , unitless) factor.

$$dB_{f\_degr} = B_{f(t-1)} e^{-PDR_{flat} fT_{flat} fW_{flat} fCN_{flat} fContact_{flat}} \quad [9]$$

All the limiting factors included are unitless and range between 0 and 1.

The moisture factor (Eq. 10) represents surface layer soil water content ( $SWC$ , m<sup>3</sup> m<sup>-3</sup>) influence on flat residue wetness and therefore on their decomposition rate. The moisture factor included in the integrated mulch model of ARMOSA differs from the one employed in APSIM.

The modification was performed to use the moisture limiting factor equation both for flat surface and buried residue decomposition.

$$fW_{flat} = \begin{cases} 0 & \text{when } SWC < SWC_{min} \\ MA_{min} + (1 - MA_{min}) \frac{(SWC - SWC_{min})}{(SWC_{optmin} - SWC_{min})^{MA_{optb}}} & \text{when } SWC < SWC_{optmin} \\ 1 & \text{when } SWC < SWC_{optmax} \\ MA_{sat} + (1 - MA_{sat}) \frac{(SWC_{sat} - SWC)}{(SWC_{sat} - SWC_{optmax})^{MA_{opta}}} & \text{else} \end{cases} \quad [10]$$

The temperature factor (Eq. 11) is obtained as a function of daily average air temperature ( $T_{avg}$ , °C) and is defined by a optimum decomposition temperature parameter ( $T_{opt}$ , °C).

$$fT_{flat} = \begin{cases} \left(\frac{T_{avg}}{T_{opt}}\right)^2 \\ 0 & \text{if } T_{avg} < 0 \end{cases} \quad [11]$$

The carbon to nitrogen ratio factor (Eq. 12) of a specific flat residue type is calculated as a function of the C:N ratio of the residue ( $CN$ , unitless) that is defined by three parameters: the optimum C:N ratio for

decomposition ( $CN_{opt}$ , unitless), the function slope coefficient ( $CN_{slope}$ , unitless) and the C:N ratio value above which the decomposition stops ( $CN_{max}$ , unitless).

$$fCN_{flat} = \begin{cases} \exp\left(\frac{-CN_{slope}(CN - CN_{opt})}{CN_{opt}}\right) & \\ 1 \text{ if } CN < CN_{opt} & \\ 0 \text{ if } CN > CN_{max} & \end{cases} \quad [12]$$

The contact factor (Eq. 13) describes the effect of the flat residue biomass amount on the soil-residue contact degree and therefore on residue decomposition rate, since lower amount of residue biomass decomposes faster due to their higher contact degree with soil. This limiting factor is estimated as a function of flat residue biomass ( $B_f$ , kg DM m<sup>-2</sup>) defined by a critical residue biomass parameter ( $B_{f\_crit}$ , kg DM m<sup>-2</sup>) The critical residue biomass is the value above which the decomposition is slowed down by the “haystack effect” described by Thorburn et al. (2001), which does not consider standing residue contribute.

$$fContact_{flat} = \begin{cases} 1 & \text{if } B_f < B_{f\_crit} \\ \frac{B_{f\_crit}}{B_f} & \text{if } B_f > B_{f\_crit} \end{cases} \quad [13]$$

The conversion of standing residue to flat residue caused by weather events such as wind and snow respectively decreases standing residue (Eq. 14) and increases flat residue amounts. It is simulated by means of WEPP approach. that employs an adjustment factor ( $Conv_{fct}$ , unitless) representing the fraction of standing residue not converted to flat residue from wind and snow for the considered site.

$$dB_{s\_conv} = 1 - Conv_{fct} B_{s(t-1)} \quad [14]$$

Surface flat residue water dynamics are simulated adopting STICS approach, which estimates the amount of water both intercepted and directly evaporated by the mulch layer.

The amount of water which is intercepted by the mulch layer ( $WC_{mulch}$ , Eq. 15) is the incident effective rainfall reaching the mulch layer (consisting in rainwater minus the amount intercepted by canopy of the crop). The intercepted water is simulated as a function of surface residue biomass ( $B_f$ , kg DM m<sup>-2</sup>) defined by one parameter representing the residue wettability ( $WETT_{mulch}$ , mm Mg ha<sup>-1</sup>). According to Scopel et al. (1998), the residue wettability depends on residue size resulting from different management operations and ranges between 0.22 and 0.38 mm Mg ha<sup>-1</sup>.

$$WC_{mulch(t)} = WETT_{mulch} B_{f(t)} \quad [15]$$

The mulch evaporation demand (Eq. 16) is estimated based on STICS approach multiplying the evaporation demand ( $EVAP_d$ , mm) by the actual soil fraction covered by flat residue ( $C_{total\_actual}$ , unitless).

$$E_{mulch} = EVAP_d C_{total\_actual} \quad [16]$$

The soil evaporation is adjusted subsequently to fulfil the unsatisfied evaporation request.

The soil cover due to surface residue presence is simulated through WEPP approach, that estimates the total soil cover due to residue presence ( $C_{total}$ , Eq. 17) as the sum of two components: flat residue ( $C_{flat}$ , Eq. 18) and



standing residue ( $C_{stand}$ , Eq. 19) soil cover. The soil covering effect is expressed as the fraction of surface covered by the residues and ranges from 0 to 1.

$$C_{total(t)} = C_{flat(t)} + C_{stand(t)} \quad [17]$$

Soil cover due to flat residue is simulated as a function of its biomass using a crop specific parameter ( $rtC_{flat}$ ,  $m^2 kg^{-1}$ ) representing the surface covered by a fixed amount of the specific crop residue.

$$C_{flat(t)} = 1 - e^{-rtC_{flat} B_f(t)} \quad [18]$$

Soil cover due to standing residue is estimated as a function of the ratio between the standing residue biomass at the considered time step and the standing residue at harvest ( $B_{s(0)}$ ,  $kg DM m^{-2}$ ). This function involves a crop specific parameter ( $A_{bm}$ , unitless) describing the surface occupied by stem basal area at maturity per square metre of soil.

$$C_{stand(t)} = \frac{B_s(t)}{B_{s(0)}} A_{bm} \quad [19]$$

Tillage operations have two main effects on the mulch biomass, both depending on the tillage type and intensity. The first one is to transfer a fraction of the standing residue to the flat residue. The second effect is the incorporation of a fraction of the flat residue into the soil; this process creates pools of organic matter that will evolve independently during the simulation.

The albedo of soil as influenced by both standing and flat surface residue presence is simulated adopting an approach derived from STICS. Soil albedo ( $ALB_s$ , unitless, Eq. [20]) is simulated as a function of the soil cover due to surface residue presence ( $C_{total}$ , unitless). The parameter involved in the function are the ones describing dry soil albedo ( $ALB_{bare}$ , unitless), mulch albedo ( $ALB_{mulch}$ , unitless).

$$ALB_{s(t)} = ALB_{bare} \times (1 - C_{total(t)}) + ALB_{mulch} \times C_{total(t)} \quad [20]$$